JCTC Journal of Chemical Theory and Computation

Article

pubs.acs.org/JCTC

Applicability of Quantum Thermal Baths to Complex Many-Body Systems with Various Degrees of Anharmonicity

Javier Hernández-Rojas,*[,†] Florent Calvo,[‡] and Eva Gonzalez Noya[§]

[†]Departamento de Física and IUdEA, Universidad de La Laguna, 38205, La Laguna, Tenerife, Spain

[‡]Laboratoire Interdisciplinaire de Physique, Rue de la Piscine, Campus Saint Martin d'Hères, 38000 Grenoble, France

[§]Instituto Química-Física Rocasolano, Consejo Superior de Investigaciones Científicas, Calle Serrano 119, 28006 Madrid, Spain

Supporting Information

ABSTRACT: The semiclassical method of quantum thermal baths by colored noise thermostats has been used to simulate various atomic systems in the molecular and bulk limits, at finite temperature and in moderately to strongly anharmonic regimes. In all cases, the method performs relatively well against alternative approaches in predicting correct energetic properties, including in the presence of phase changes, provided that vibrational delocalization is not too strong—neon appearing already as an upper limiting case. In contrast, the dynamical behavior inferred from global indicators such as the root-mean-square bond length fluctuation index or the vibrational spectrum reveals more marked differences caused by zero-point energy leakage, except in the case of isolated molecules with well separated vibrational modes. To correct for such deficiencies and reduce the undesired transfer among modes, empirical modifications of the noise power spectral density were attempted to better describe thermal equilibrium but still failed when used as semiclassical preparation for microcanonical trajectories.

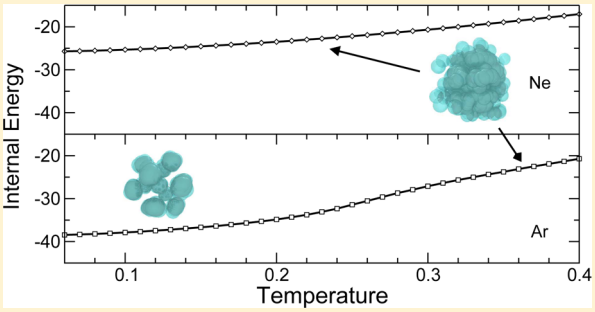

1. INTRODUCTION

As the primary manifestation of nuclear quantum effects in atomic and molecular systems, vibrational delocalization becomes important below the Debye temperature and may impact structural, thermal, or dynamical properties. One current challenge faced by theoretical and computational chemistry deals with the inclusion of such effects in particle-based simulations, given that the nuclear Schrödinger equation can only be solved exactly for low-dimensional systems. Due to the poor scaling of wavepacket-based methods in high dimensions, approaches such as vibrational configuration interaction[1] or vibrational self-consistent[2] field have been limited to molecular scales so far, similar limitations existing for promising strategies relying on Gaussian wavepackets.[3,4] Various alternative approaches have been proposed to account for nuclear quantum effects. Semiclassical ideas in which delocalization is mimicked by distributing initial conditions in trajectory-based methods date back to Wigner and have been pursued notably by the Miller[5,6] and Makri[7,8] groups, among others.[9,10] Reciprocal methods, in which the information from classical simulations is postprocessed by quantum corrections,[11,12] also fall into this class. A more rigorous framework is provided by imaginary time path-integrals,[13−16] which in the context of time correlation functions builds on two main families of centroid molecular dynamics (CMD) of Voth and co-workers[17,18] and more recently ring-polymer molecular dynamics (RPMD) developed by Manolopoulos and co-workers.[19,20] Hybrid approaches combining the most prominent features of semiclassical preparation and path-integral (PI) methods have also been proposed, as in the recent Liouville dynamics[21] that allows time correlation functions to be evaluated for nonlinear operators.

One approximate method which has gained momentum over the past few years owing to its relative simplicity and strong connection with well-established semiclassical ideas is quantum thermal baths (QTBs).[22−28] The QTB approach consists of propagating the phase space variables within a Langevin equation formalism, using a correlated (colored) noise instead of the traditional white noise as in classical Langevin MD. The introduction of a colored noise, which may be Markovian[28] or not,[27,29] aims to mimic the different response of vibrational modes in quantum mechanics and the ability of those modes to store some zero-point energy. Since its introduction the method has been applied to a variety of problems in chemical physics including energy transfer and thermal conductivity,[30−33] isotopic effects in materials,[34] shock compression at low temperatures,[35] or the evaluation of vibrational delocalization in molecular systems.[36−38] It has also been suggested a useful addition to path-integral molecular dynamics (PIMD),[39] modified into a deterministic version with Nosé−Hoover thermostatting schemes,[40] and was recently shown of potential interest for specific computational tasks.[41]

Received: July 29, 2014

DOI: 10.1021/ct500678z
J. Chem. Theory Comput. XXXX, XXX, XXX−XXX

The main appeal of the QTB approach lies in its computational cost that is comparable to classical molecular dynamics and does not scale defavorably with an increasing degree of delocalization. Although its utility has been recognized in the aforementioned works, its approximate character has been duly noted, in particular in the presence of anharmonicities.[42,43] In addition, and as with other semiclassical preparation methods, it is prone to zero-point energy leakage, a problem in which high-frequency modes flow into softer degrees of freedom.[44,45] Different attempts to correct for this deficiency have been proposed, based on generating differently colored noise spectra or memory kernels in the numerical solution of the Langevin equation.[32,40] In the non-Markovian approach of Ceriotti and co-workers,[27,39] the procedure is rather tedious and requires tuning the noise function to constrain the energy drift among modes. The deterministic approach of Ganeshan and co-workers uses a simpler strategy but requires knowledge of the vibrational spectrum.[40] Finally, Bedoya-Martínez and co-workers have directly modified the noise power spectrum in order to reach self-consistency in the distribution of energy per mode in weakly anharmonic (nearly crystalline) systems.[32]

In the case of strongly anharmonic systems such as normal fluid helium, Dammak and co-workers found evidence that QTBs are at least semiquantitative.[28] Applications to isolated molecules also compared reasonably well with reference data.[36,38] This raises the question of the relevance of the QTB approach for simulating atomic or molecular systems across regimes where anharmonicities strongly vary, as in the case of phase changes. Phase transitions, both of first- and second-order, are notoriously difficult to simulate by conventional algorithms because of the extra effort needed to cross the nucleation barrier to the other phase and circumvent hysteretic phenomena, incidentally explaining the popularity of quantum correcting schemes such as Feynman−Hibbs[46] or Kirkwood−Wigner[47,48] approaches for addressing this issue. The interest to have particularly efficient methods to account for quantum effects also in the case of phase changes has motivated us to consider QTBs and determine how they perform in this context. More generally, we wish to examine to which extent the global statistical equilibrium and even dynamical features are captured by QTB methods for different atomic and molecular systems.

In the present article, we have carried out a comprehensive investigation of stochastic QTBs in various anharmonic regimes governed by the interactions and masses as well as external temperature or density. Lennard-Jones (LJ) finite clusters and periodic bulk samples provide suitable candidates for addressing the importance of nuclear delocalization through a systematic comparison of the behaviors of argon and neon. Water in isolated and cluster form was chosen as our second testing case, giving more insight into the importance of zero-point energy leakage arising from energy flow between intra- and intermolecular modes. Our implementation of QTBs was taken from the portable version of the original method by Dammak and co-workers,[28] as proposed by Barrat and Rodney.[49] To assess the performance of the method on quantitative grounds, path-integral Monte Carlo (PIMC) and PIMD have been carried out for comparison as well as quantum[50] harmonic superposition calculations.[51] Without altering the noise power spectrum, the QTB method is generally found to lead to rather satisfactory energetic properties in all cases, especially away from phase changes regions. However, the signatures of the phase changes themselves are not reliable, a result that hides a more severe issue in the breaking down of the semiclassical approximation already in the case of neon. A similar deceptive result is found for water clusters, which due to strong zero-point energy leakage are found to be floppy down to low temperatures (even at 0 K!), a result that again is not apparent from purely energetic considerations. Despite these limitations, the method is found to produce vibrational properties that are rather consistent with PI data, even in the case of zero-point energy leakage where PI methods themselves are problematic in this context. The relative broadenings in the vibrational peaks are at greater variance with benchmark data, suggesting those properties to be a more robust indicator of inaccurate sampling with the QTB method. Empirical modifications of the noise generating function to limit zero-point energy leakage to low-energy modes by favoring high-energy degrees of freedom were attempted, but with moderate success; correcting for global phase behavior could not be achieved without degrading the energetic properties.

The article is organized as follows. In the next section we briefly describe the way QTBs have been used in the present work and give some details about the alternative methods employed for comparison. Our results on rare-gas clusters and bulk samples are presented and discussed in Section 3, before the molecular case of water is discussed. Some concluding remarks are finally given in Section 4.

2. METHODOLOGY

2.1. Quantum Thermal Baths (QTB). A fairly recent methodology to incorporate nuclear quantum effects consists of placing the system in contact with a thermal bath with appropriate colored (or correlated) noise, also called QTB.[22−28] Here the specific approach of Dammak and co-workers[28] was adopted, as it is perhaps the simplest and least dependent on adjustable parameters. The dynamics obeys the Langevin equation with a random force and a dissipation term related to each other through the quantum fluctuation−dissipation theorem. The power spectral density (PSD) is related to the damping constant γ and to Bose−Einstein distribution including the zero-point energy.[28] In other words, we have a Langevin equation with a colored noise where the vibrational energy of the system obeys a Bose−Einstein spectrum. In the classical limit $\hbar \to 0$, the particles move in phase space following a canonical trajectory with white noise, and the PSD is independent of frequency and equals $k_B T$.

To calculate the random forces, we use the portable version of Barrat and Rodney,[49] which avoids generating and storing all random forces before the simulation and also avoids calculating the inverse Fourier transforms at each new time step. This algorithm is based on an appropriate linear filter applied to a white noise, the correlated noise $\theta(t)$ being calculated by convoluting the discrete Fourier transform of the filter with a Gaussian white noise signal.[49] Here the random noise signal was updated with a time period of $\Delta t \approx \pi/\Omega_{max}$, and the power spectrum is discretized into $2N_f$ bins in the range $-\Omega_{max} \le \omega \le \Omega_{max}$.[49]

Practical integration of the Langevin equations of motion was achieved using the Brünger−Brooks−Karplus (BBK) algorithm,[52] however additional tests were conducted with the so-called symplectic low-order (SLO) algorithm.[53] Comparisons between the two methods are discussed in the Supporting Information.

DOI: 10.1021/ct500678z
J. Chem. Theory Comput. XXXX, XXX, XXX−XXX

2.2. Alternative Approaches. *2.2.1. Path-Integral Monte Carlo (PIMC) Simulations.* Nuclear quantum effects can be rigorously incorporated in Monte Carlo (MC) simulations using the PI formalism.[46] In this approach the canonical partition function of a system of N quantum particles is functionally identical to that of a classical system of N ring polymers with P beads (or replicas).[54,55] Each bead interacts with the adjacent beads in the same ring through harmonic springs and with the same bead of the remaining rings through the physical potential. The spring constant of the harmonic potential depends on the mass of the particles, the temperature, and the number of replicas. This isomorphism allows to use all the classical formalism to perform quantum simulations that sample the configurational space described by the partition function and to calculate average properties along those simulations.[54,55]

The PI formalism is strictly exact only when an infinite number of replicas is used. However, in practice, the number of replicas is chosen large enough to capture accurately the quantum effects but small enough to keep the problem computationally tractable.[56] Indeed, it is generally accepted that the main contribution to quantum effects are captured by taking $P > \hbar\omega/k_BT$, ω being the maximum vibrational frequency of the system. In order to have a similar error independently of temperature, the product PT was kept constant for each system. For LJ clusters we used $PT = 1$ for argon and $PT = 3$ for neon, T being the reduced temperature in this case. The water monomer was studied using $PT = 6000$ K (corresponding to $P = 120$ at $T = 50$ K and $P = 20$ at 300 K) and $PT = 12\,000$ K (i.e., $P = 240$ at $T = 50$ K and $P = 30$ at $T =$ 300 K). These numbers of replicas are similar to those used in previous works.[57] The availability of results for two different number of replicas at each temperature will allow us to check the convergence of the internal energy with the numbers of replicas. For the water octamer we then used $PT = 12\,000$ K.

PIMC simulations included several types of MC moves to ensure a proper sampling of all degrees of freedom. For the rare-gas clusters, a simulation cycle consisted of NP attempts to displace one replica of one atom, plus another N attempts to displace or rotate a whole ring. In the case of the water clusters, a simulation cycle consisted of $3N_{mol}P$ attempts to displace one replica of one atom, $N_{mol}P$ attempts to displace or rotate one replica of one molecule, $3N_{mol}$ attempts to displace or rotate the whole ring of one atom, and N_{mol} attempts to displace or rotate all replicas of one entire molecule, with N_{mol} being the number of water molecules. Typically simulations consisted of about 10^7 MC cycles for equilibration plus about 5×10^7 to 10^8 MC cycles for taking averages.

Besides the internal energy, the Lindemann index (δ), which is often used to characterize phase transitions,[58] was also evaluated:

$$\delta = \frac{2}{N(N-1)} \sum_{i=1}^{N-1} \sum_{j=i+1}^{N} \frac{\sqrt{\langle r_{ij}^2 \rangle - \langle r_{ij} \rangle^2}}{\langle r_{ij} \rangle} \quad (1)$$

where r_{ij} is the distance between atoms i and j averaged over the P replicas.

All PIMC simulations were performed using Cartesian coordinates.

2.2.2. Path-Integral Molecular Dynamics (PIMD) Simulations. We also wish to challenge QTBs in the context of dynamical or transport properties, aiming to question whether the method can indeed produce suitable semiclassical approximations of the quantum wave function. The PI framework described previously does not provide any direct information about time-dependent properties, but the CMD and RPMD dynamical versions of PIMD offer alternative benchmarks.[18,20] We have carried out such simulations in order to evaluate the vibrational or infrared (IR) spectra from the Fourier transform of the velocity or electric dipole moment, respectively. The implementation and use of such methods in the context of vibrational spectroscopy has been recently reviewed by Pérez and co-workers,[59] and we follow the standard procedure here by first producing a sample of thermostated phase space configurations at fixed temperature through massive use of Nosé−Hoover variables coupled to all normal mode coordinates of the system. These configurations are subsequently propagated without thermostat, recording the observables of interest for further processing.

PIMD simulations were carried for rare-gas samples (bulk and clusters) as well as the water monomer and octamer modeled by the q-TIP4P/F model. For the rare gases the temperature was fixed at $T = 0.1$ reduced units, the Trotter discretization number being taken as $P = 12$ for argon and $P = 36$ for neon. Additional simulations for $P = 4$ (argon) and 12 (neon) were performed as well in order to illustrate the effects of Trotter convergence (results given as Supporting Information). Time steps of 10^{-3} and 5×10^{-3} reduced units were employed for partially adiabatic CMD (PA-CMD) simulations with and without thermostatting, the adiabatic parameter being chosen in order to damp frequencies higher than 30 reduced units. The RPMD trajectories used a time step of 5×10^{-3}.

For water, the PIMD simulations were conducted at $T = 50$ K and $P = 100$ in order to facilitate comparison with the recent work by Videla and co-workers[60] who already studied nuclear quantum effects in the dynamics of the q-TIP4P/F water octamer. The time steps for canonical sampling were taken as 0.02 and 0.1 fs for the PA-CMD and RPMD trajectories, respectively, and the adiabatic parameter of PA-CMD simulations was taken in order to damp frequencies higher than 5000 cm^{-1}. A common time step of 0.1 fs was used for the subsequently propagated microcanonical trajectories. Again, additional simulations were carried out at a lower value of $P = 10$ to give insight into the effects of Trotter discretization, the results being given as Supporting Information.

All PIMD simulations were propagated using normal mode coordinates and nonthermostated trajectories integrated with the reference system propagation algorithm method.[61]

2.2.3. Harmonic Superposition Approximation (HSA). In addition to PIMC and PIMD simulations, the thermal properties at equilibrium were also evaluated using an approximate but efficient scheme in which the partition function is constructed by appropriate summation over a set of known isomers.[51] Thus, the partition function indicates a quantum mechanical description of vibrations, resulting in what will be referred to as the quantum superposition method or QSA.[50] In the limit $\hbar \to 0$ the partition function simplifies into the known expression for classical partition function. The method is particularly useful in the quantum case because unlike PI methods it does not suffer from the divergence in Trotter discretization at low temperatures. The main approximations are thus the neglect of tunneling, the harmonic description of vibrations, and the need for a representative sample of minima. Although anharmonicities can be accounted

DOI: 10.1021/ct500678z
J. Chem. Theory Comput. XXXX, XXX, XXX−XXX

for through perturbative expansions,[62−64] they are not needed here as the superposition method is mainly used to capture the ranges of variations in the thermal properties accross the melting point.

The other issue of producing representative samples of minima was addressed by performing parallel tempering MC trajectories and systematically quenching the configurations to their closest minima. 11,072 minima were thus obtained for the q-TIP4P/F water octamer and 1415 for the 13-atom LJ cluster. From the expression of the partition function, the internal energy is straightforwardly obtained, but the method does not provide any direct insight into time-dependent properties, the dynamics, and is thus unable to evaluate the Lindemann index.

3. RESULTS AND DISCUSSION

Anharmonicities develop very differently in atomic and molecular systems owing to the separation of frequencies in the latter, where zero-point energy leakage problems can be particularly severe due to unphysical mixing between intra- and intermolecular modes in semiclassical descriptions. The performance of QTBs in systems with increasing anharmonic behaviors is first discussed in rare-gas many-body systems, before turning to the more complicated case of water clusters.

3.1. Lennard-Jones (LJ) Systems. In reduced LJ units, the various rare gases differ in terms of vibrational delocalization from the value of the Planck constant, which is then known as the dimensionless de Boer parameter $\Lambda = \hbar/\sigma(m\varepsilon)^{1/2}$, ε and σ being the LJ parameters and m the atomic mass. For classical, argon, and neon systems Λ takes values of 0, 0.03, and 0.095, respectively. The Langevin MD simulations for these clusters were performed with a time step of 7.15×10^{-3} and a damping factor of $\gamma = 10^{-2}$. The effects of the damping constant were specifically investigated, and the results obtained using alternative values of γ given as Supporting Information. In the present range of parameters, the thermodynamical properties are stable against variations of the damping factor of about 1 order of magnitude. The QTB parameters were taken as $\Omega_{max} = 50$ and $N_f = 200$. We used 40 temperatures regularly spaced in the range $0.01 \leq T \leq 0.4$. The Langevin MD trajectories were propagated for 5×10^6 time steps, averages being accumulated after 10^5 steps. In order to reduce fluctuations, all results were averaged over five independent trajectories.

QTB methods being initially devoted to mimicking the effects of nuclear delocalization on equilibrium properties, we first consider the internal energy $U(T)$ as the main quantity of interest, for the rare-gas clusters LJ_n, Ar_n, and Ne_n with $n = 13$, all studied in the same reduced temperature range $0.05 \leq T \leq 0.40$ that contains the melting point for all three systems.[50] In Figure 1 we show the results obtained with classical or QTBs, compared with MC or PIMC benchmark results as well as data obtained with the harmonic superposition approximation. The results obtained in the classical case are in very good agreement with each other, the HSA underestimating the internal energy at high temperature due to its neglect of basin anharmonicities.[50,62] In particular, the Langevin MD and classical MC approaches both reproduce the known inflection in the internal energy near $T \simeq 0.28$ that indicates melting.[58]

The quantum nature of argon remains very moderate in this temperature range, and the QTB method is able to reproduce part of the other reference results, namely, the correct internal energy in the solid-like state. Near the melting region $T \sim 0.25-0.28$ and beyond, the QTB method slightly

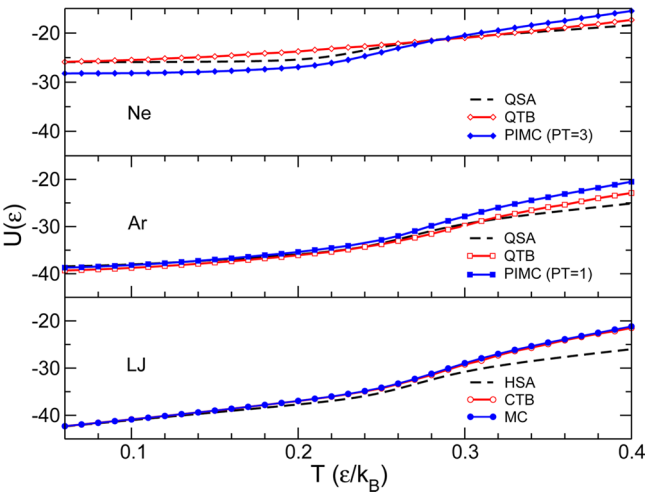

Figure 1. Internal energy of 13-atom rare-gas clusters in the classical limit (LJ, lower panel) and corresponding to argon (middle panel) and neon (upper panel), as obtained using classical (CTB) and QTBs, PIMC, and the harmonic superposition methods (HSA and QSA).

underestimates $U(T)$, and the superposition approach (QSA) produces the same result.

At this stage QTBs seem at least semiquantitative and even able to treat strongly anharmonic regimes, but in a mildly quantum system for which vibrational delocalization can be considered as a correction on top of an essentially classical behavior. The Ne_{13} cluster offers a more challenging case, not as extreme as a helium droplet but still expected to display much stronger delocalization and zero-point shift than in argon.[50,65,66] This is indeed what the three computational methods predict, with an increase in internal energy at low temperature by more than 10 LJ units. For this system, the variations in internal energy are much smoother than for argon, although a melting range near $T \sim 0.24$ can still be discerned for the PIMC and superposition methods, in agreement with earlier studies.[50,65,66] At low temperature, the PI simulation may not be fully converged in terms of Trotter discretization number, causing some underestimation in the internal energy. Similar differences between PIMC (using a much larger discretization number $P = 300$) and the harmonic approximation were previously noted[67] but could be also due to some breakdown of the harmonic approximation itself already at low temperatures, as reflected on the redshift often exhibited by fundamental frequencies with respect to harmonic values. Such anharmonicities of the ground-state vibrational wave function could lead to some significant overestimation of the zero-point energy in the harmonic approximation.[68] While the QTB method seems to be in reasonable agreement in the overall temperature range, it does not show a clear inflection acting as a signature of melting.

To interpret this seemingly minor discrepancy we turn to another indicator of the global dynamics, namely the Lindemann index δ. The variations of this property have been represented in Figure 2 as a function of temperature for the three clusters, as obtained from the PIMC and thermal bath simulations. For the three systems, the PI calculations predict relatively smooth variations in δ both at low and high temperatures, with a markedly strong increase in a narrow temperature range lower than the melting range. Whereas δ does usually provide a convenient observable to define melting points from simulations,[58] it is actually less relevant for the 13-

DOI: 10.1021/ct500678z
J. Chem. Theory Comput. XXXX, XXX, XXX−XXX

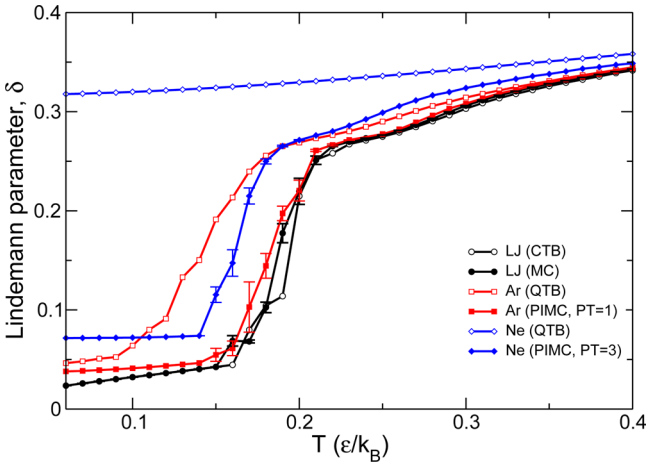

Figure 2. Root-mean-square bond length fluctuation index for 13-atom rare-gas clusters in the classical LJ limit and corresponding to argon and neon, as obtained using classical (CTB) and QTB and classical (MC) and PIMC.

atom LJ cluster, which undergoes some highly fluxional motion involving permutational isomers of the exceptionally stable icosahedral global minimum, but none of the other minima.[58] Putting this peculiarity aside, the temperature at which the Lindemann index strongly increases and its dependence on the de Boer parameter is consistent with the temperature range where the internal energy exhibits a curvature change in Figure 1.

While the classical and argon clusters are both solid-like at low temperatures in the QTB simulations, the neon cluster appears to be fluid-like ($\delta > 0.3$) already at $T = 0.05$ reduced units, and repeating the simulations below this temperature confirms that this system does not remain rigid. This is consistent with the absence of any signature for a phase change on the internal energy, despite correct overall energetics. The inability of the QTB method to capture both the energetics *and* the physical state of the system can be explained by noticing that at a total energy close to -26ϵ (as indicated in Figure 1) the cluster is able to cross several low-energy barriers leading to minima other than the icosahedron.[69] This microcanonical picture is relevant to the QTB approach, which is semiclassical and lacks correlations between positions and momenta. This deficiency causes unphysical combinations and excessive kinetic energies concomitant with higher-lying regions of the potential energy surface, causing in turn such spurious melting phenomena.

The failure of QTBs to keep the neon cluster rigid-like at low temperatures was not fully expected, because when applied to bulk helium the method correctly predicts a fluid state.[28] This lead us to consider bulk rare gases as well, taking a 256-particle system with periodic boundary conditions and initially on the face-centered cubic (fcc) lattice, at the fixed density of 1.08 reduced units and temperature $T = 0.1$. The QTB method finds internal energies of $U = -8.1$, -7.6, and -6.0 ϵ/atom for the classical, argon, and neon cases, respectively, in good agreement with the harmonic and PIMD values. For these bulk systems, the Lindemann indices are now all below 0.1, indicating that the QTB method produces equilibrated samples in the correct crystal phase. The reason why the method works satisfactorily here is to be found in the greater energies needed to melt the bulk system, which lacks the free surfaces where the cluster could easily produce defects and nucleate the liquid around them.

The Lindemann index being only a global indicator, we have considered a more detailed property of the underlying dynamics as the vibrational spectrum, obtained from the Fourier transform of the velocity time correlation function and evaluated here at the Γ point of the first Brillouin zone:

$$I(\omega) \propto \int_{-\infty}^{+\infty} \langle \vec{v}(0)\cdot\vec{v}(t)\rangle e^{-i\omega t} dt \qquad (2)$$

The spectra obtained from classical MD trajectories prepared with initial conditions sampled by classical and QTBs, as well as their comparison with PI spectra in the ring-polymer and partially adiabatic centroid MD frameworks, are depicted in Figure 3 for the LJ, argon, and neon cases.

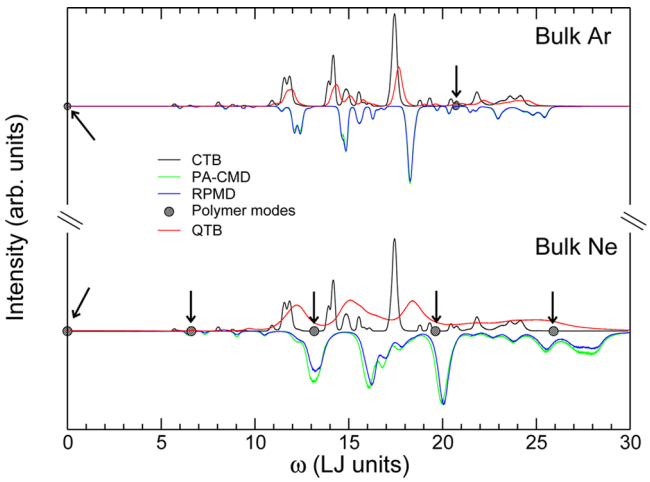

Figure 3. Power spectrum of the velocity time autocorrelation function for bulk LJ samples corresponding to argon or neon at the reduced density 1.08 and temperature 0.1, respectively, as obtained from classical or PI (RPMD and PA-CMD) molecular dynamics. The initial conditions of the classical MD trajectories were prepared using CTB and QTB. The intrinsic polymer modes for Ar ($P = 12$) and Ne ($P = 36$) are depicted as well and indicated by arrows.

The spectra for argon and neon are of course identical when simulated with the classical thermal bath and show a series of peaks corresponding to the most active phonon modes. The high symmetry of the fcc lattice makes the vibrational spectrum particularly well resolved, consistent with the rigid character of the system at low temperature already inferred from the Lindemann index. The vibrational spectrum of the solid argon sample obtained with the PI methods is very similar to the classical spectrum, except for a general blue shift of the peaks due to anharmonicities. It is worth noting that for this system the two PIMD methods agree well with one another, even at frequencies higher than one ring-polymer mode near $\omega \sim 20.5$ LJ units. In comparison the classical spectrum initiated from QTB phase space points looks intermediate between the classical and PI spectra in terms of band positions and intensities, but with clearly broader peaks often merging closeby lines. Using damping constants larger than 10^{-2} in the Langevin MD simulations yields even broader spectra in the case of neon (see Supporting Information).

Vibrational delocalization in solid neon causes much stronger blue shifts and broader peaks, as seen from both PIMD spectra that again satisfactorily agree with each other. Even though the

DOI: 10.1021/ct500678z
J. Chem. Theory Comput. XXXX, XXX, XXX−XXX

spectrum is made of fewer but broader bands, it remains clearly that of a solid with no apparent diffusion indicated by a positive value at low ω. The same qualitative result holds for the classical spectrum obtained with QTB-prepared initial conditions, but as was the case for argon the spectral features appear exceedingly broad and only the four peaks that contribute most to the spectrum are distinguishable near ω = 12.4, 15.1, 19.0, and $\omega \sim 23-36$, without any better resolution.

Excessive broadenings produced by the QTB method were previously noted in the related case of molecular IR spectra,[36] but they are found to be particularly salient here, preventing a clear identification of individual peak locations. Therefore, despite the good quantitative agreement on the energetics and the equally good qualitative agreement about the solid nature of the equilibrium phase, finer details of the dynamics are not correctly captured by QTBs. Clearly these deficiencies are again caused by the semiclassical character of the method, most likely through the problem of zero-point energy leakage, but they are important as they more generally impact other transport properties such as thermal conductivity or expansion coefficients.

3.2. Water Clusters. Langevin MD simulations with classical or QTBs were propagated for the water monomer and octamer using a time step of 0.2 fs and a damping constant of $\gamma = 10^{-3}$ fs^{-1}. The noise was generated using parameters of $N_f = 200$ and $\Omega_{max} = 8000$ cm^{-1}. Forty temperatures regularly spaced in the range $50 \leq T \leq 300$ K were performed. The Langevin MD trajectories were integrated for 5×10^7 time steps, averages being acumulated after 2×10^5 steps. All results were averaged over three independent realizations of initial conditions. The sensitivity of some results on the damping factor, as discussed in greater length in the Supporting Information, appears negligible for the octamer and only shows some minor vibrational shifts for the monomer.

Molecular compounds are particularly sensitive to the problem of zero-point energy leakage due to the large separation usually found between intra- and intermolecular vibrational modes. In order to assess the behavior of the QTB method for molecular clusters, it is useful to evaluate its performance for individual molecules, and we have first considered the case of H_2O modeled using the q-TIP4P/F potential. For this system large-scale benchmark PIMC simulations could be performed in a broad temperature range and for high Trotter numbers. The internal energies obtained using this method are represented in Figure 4 and compared to the predictions of the approaches based on classical and QTBs. The first observation is that using a number of replicas according to the criteria PT = 6000 K is not fully sufficient to accurately predict the internal energy of the water monomer, the internal energy obtained using PT = 12 000 K being about 0.75 kcal/mol higher than that obtained with PT = 6000 K. For this simple example, the QTB method quantitatively reproduces the PIMC internal energy and accurately predicts the zero-point shift specially taking into account that it is likely that the PIMC simulations have not fully converged as a function of the Trotter number. Above 300 K anharmonicities of the potential energy surface are manifested on the quantum MC data, but they are probably underestimated by the QTB approach.

The IR absoption spectrum is evaluated from the Fourier transform of the dipole moment time autocorrelation function as[59]

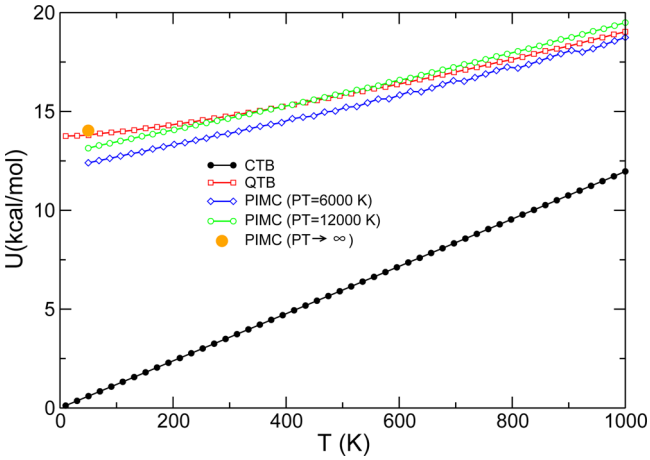

Figure 4. Internal energy of the q-TIP4P/F water monomer described by CTB and QTBs as well as PIMC, as a function of temperature.

$$I(\omega) \propto \frac{\beta\hbar\omega^2}{1 - \exp(-\beta\hbar\omega)} \int_{-\infty}^{+\infty} \langle \vec{\mu}(0)\cdot\vec{\mu}(t)\rangle e^{-i\omega t} dt \quad (3)$$

$\vec{\mu}$ being the dipole moment of the water molecule. In the previous equation the standard harmonic correction factor was used to correct for the approximation made when replacing the Kubo-transformed quantum time correlation function by its classical counterpart.[59]

The IR spectrum of the same water monomer obtained from trajectories prepared with classical or QTBs at T = 50 K is depicted in Figure 5 and compared with the results of RPMD

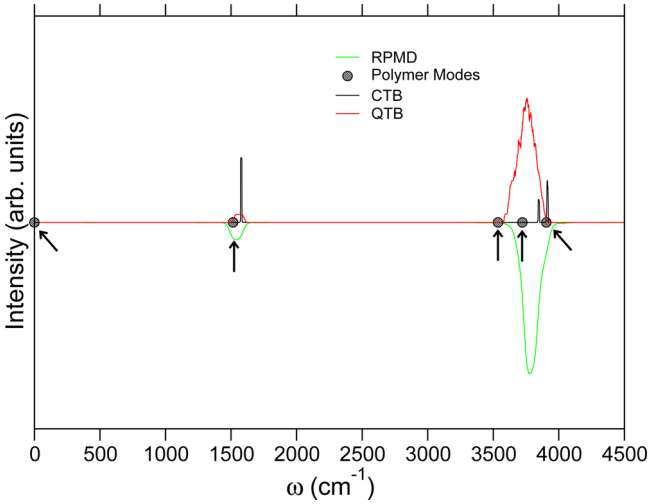

Figure 5. IR absorption spectrum of the q-TIP4P/F water monomer at T = 50 K obtained from classical or RPMD. The initial conditions of the classical MD trajectories were prepared using CTB and QTB. Intrinsic modes are indicated by arrows.

PI simulations. For this system the RPMD method displays interferences of O−H stretching modes with the intrinsic polymer modes, but the PA-CMD method turns out to produce unrealistically large redshifts[70] and was omitted from this comparison. At the very low temperature considered, the three IR active modes appear as narrow lines. According to the PIMD results, vibrational delocalization is significant and has the effect of redshifting and especially broadening those peaks to the extent of merging them in the O−H stretching region. Those

DOI: 10.1021/ct500678z
J. Chem. Theory Comput. XXXX, XXX, XXX−XXX

data are consistent with earlier similar conclusions reported by Witt and co-workers.[70] The QTB method satisfactorily reproduces the redshifts and yields a comparably broad stretching band, despite lacking the minor peak on the blue side. In contrast, the bending mode near 1500 cm^{-1} is not sufficiently broad with respect to the RPMD result. Overall the quality of the spectroscopic properties obtained by initiating the classical trajectories by QTBs is rather satisfactory for this single molecule, confirming earlier results on larger hydrocarbons.[36]

The q-TIP4P/F water octamer has recently been investigated in detail by Videla and co-workers[60] and thus provides a convenient testing ground for the QTB method. We show in Figure 6 the temperature variations of the internal energy, as

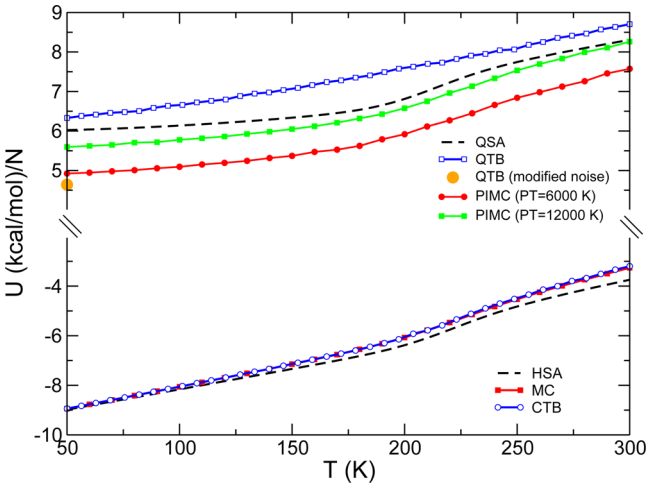

Figure 6. Internal energy of the q-TIP4P/F water octamer obtained for classical and quantum descriptions of nuclear motion from classical (CTB) and QTBs, Monte Carlo (MC and PIMC), and the harmonic superposition approximation (HSA and QSA).

obtained with both classical and QTBs and compared with the predictions of the classical and quantum HSAs and with classical and PIMC simulations. In the classical regime, the Langevin integrator quantitatively reproduces the classical MC result, which shows a steady increase of the internal energy with a minor but visible inflection near 220 K marking the center of the melting range. The classical superposition approximation confirms this value, although it underestimates the internal energy due to its neglect of anharmonicities, hence the latent heat of melting is also underestimated.

In the quantum regime, we first notice that the energy stored as zero-point motion is quite significant for this molecular system and mostly caused by the higher-frequency intramolecular modes. The low-temperature internal energy obtained with the QTB is in good agreement with the harmonic estimate, and it also agrees with the PIMC data especially considering that convergence with the Trotter number is probably not fully reached yet. The inflection signaling the phase change appears barely altered by nuclear quantum effects, and consistently among the harmonic superposition and PI calculations it lies slightly above the classical inflection point. However, the QTB method clearly misses it and significantly overestimates the internal energy in the entire temperature range. This behavior is rather similar to what was previously found for the neon cluster and can be further scrutinized by considering the global and local dynamical indicators provided by the Lindemann index (Figure 7) and the IR spectrum (Figure 8). The melting indicator δ shows the two expected regimes of flat variations at low and

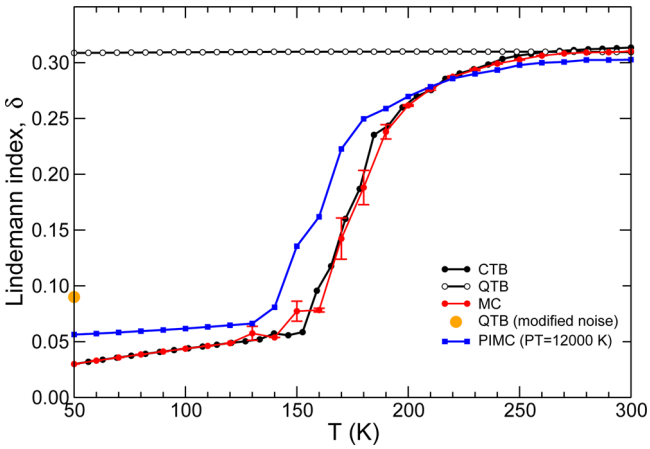

Figure 7. Intermolecular root-mean-square bond length fluctuation index for the q-TIP4P/F water octamer obtained from different classical (CTB and MC) and quantum (QTB and PIMC) descriptions of nuclear motion, as a function of temperature.

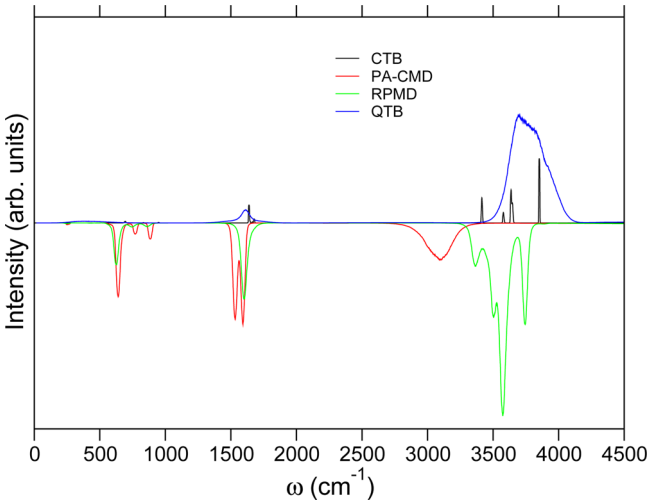

Figure 8. IR absorption spectra obtained for the q-TIP4P/F water octamer at 50 K from classical and PIMD simulations (PA-CMD and RPMD), the classical trajectories being prepared with initial conditions from CTB or QTBs.

high temperatures, corresponding to the solid-like and liquid-like phases, respectively. As was the case for rare-gas clusters, the increase in δ is a lower bound to the thermodynamical melting transition, and such an underestimation is found to be as large as 70 K in the classical case. Including nuclear quantum effects in the PI framework gives rise to a slight shift of the melting transition to lower temperatures by about 15−20 K. This two-state behavior is not reproduced by the QTB method, which predicts a fully liquid-like phase already at low temperatures.

Similarly to the case of Ne_{13} the failure of QTBs to produce the correct thermodynamical phase is again the consequence of zero-point energy leakage issues, which are especially acute for the presently coexisting van der Waals and covalent modes. Not unexpectedly, the more detailed local dynamical indicator provided by the IR spectrum reveals these flaws from another perspective. We show in Figure 8 the IR spectrum of the water

DOI: 10.1021/ct500678z
J. Chem. Theory Comput. XXXX, XXX, XXX−XXX

octamer at 50 K and in the range 0−4500 cm^{-1}, as obtained from preparations with classical and QTBs as well as RPMD and PA-CMD spectra. It should be first noted that the two PI spectra are quantitatively consistent with the recent results by Videla and co-workers[60] who also found some excessive redshift in the O−H stretching band and splitting of the H−O−H bending modes with the PA-CMD method and appearance of IR-inactive modes due to interference with the polymer modes in the RPMD method. Given those known limitations the QTB approach yields an IR spectrum that is surprisingly not so much at variance with the PIMD spectra, in the sense that it inherits broadenings that are comparable to that of PA-CMD and redshifts that are close to that of RPMD. From a quantitative perspective, the O−H stretching band and the far-IR intermolecular band differ most from the other reference results, and those differences are ascribed to the incorrect allocation of energy in the inter- and intramolecular modes, especially the latter which can store less energy than their zero-point limit due to leakage.

Comparison of the IR spectra obtained from the three methods is instructive because in absence of several reference results, all with their own intrinsic deficiencies, the QTB approach does not perform so obviously poor in terms of spectral features. From the Lindemann index we know that the system is disordered and most likely visits isomers other than the cubic ground state. One extra cause for the particularly broad spectral lines, in addition to the naturally excessive broadenings noted earlier, is thus the contribution of these other isomers that are not present in the two PI simulations.

3.3. Discussion. The problem of zero-point energy leakage with the semiclassical methods based on QTBs has been discussed before by various authors,[36,39,40] who pointed out the need of thermostatting separately the different vibrational modes in order to prevent unwanted transfer between them. Here the problem appears particulary critical because it leads to spurious melting of molecular and even atomic systems, making the method qualitatively inappropriate. The most promising results, obtained for water, unfortunately indicate that appropriate procedures based on Langevin integrators are very system-specific and far from straightforward.[39,40] In order to keep the generality of the QTB method used in the present work as much as possible, and following an earlier suggestion by Bedoya-Martínez et al.,[32] we have attempted to modify the dynamics through the spectral properties of the colored noise, favoring the high-energy modes at the expense of low frequencies and changing the PSD by the following *empirical* expression:

$$\tilde{\Theta}_{\mathrm{mod}}(\omega) = \tilde{\Theta}(\omega) \times \varphi(\omega)$$

$$\varphi(\omega) = \frac{\exp[\alpha_0(|\omega| - \omega_0)]}{1 + \exp[\alpha_1(\omega_1 - |\omega|)]} \qquad (4)$$

where α_0, α_1, ω_0, and ω_1 are adjustable parameters. The form for φ above was chosen in order to damp frequencies lower than ω_1 and enhance frequencies higher than ω_0. Bedoya-Martínez and co-workers have recently followed a similar strategy to correct for zero-point energy leakage in solid aluminum, but the noise was modified by hand in a more tedious procedure.[32] The simple approach we try here is perhaps not as general, although it hopes to capture the desired effects. Obviously, such a strategy would not be recommended in general as it is largely arbitrary and would make the QTB approach lose its attractive universal character.

The parameters of this modified noise were chosen with several objectives in mind. First, we wish to preserve the internal energy and zero-point shift as close as possible to the expected value. However, and more importantly, we also aim to preserve the thermodynamic phase expected for the system of interest and keep it solid at low temperatures. A systematic MC optimization of the parameters was thus carried out for the water octamer at T = 50 K, minimizing an error function aiming to reproduce the (harmonic) internal energy and giving the lowest possible Lindemann index δ. For this example a set of parameters meeting these constraints was obtained as α_0 = 1.792×10^{-5} cm, α_1 = 6.381×10^{-3} cm, ω_0 = 944 cm^{-1}, and ω_1 = 408 cm^{-1}, leading to a modified noise whose PSD is depicted as an inset in Figure 9. The internal energy and Lindemann index obtained with this modified noise have been superimposed in the corresponding Figures 6 and 7, respectively. Despite not being fully successful, the numerical solution obtained for this adjustment problem yields an internal energy that is off by about 1.4 kcal/mol, and a Lindemann index that is still below the approximate threshold of 0.15 for signaling the liquid, though not by a large extent. Despite relatively small modifications made on the noise, the consequences on the dynamics can thus be qualitative. However, it is likely that the actual effect of the noise modification lies in a slower energy flow from high- to low-energy modes, which under the time scale of 10 ns is sufficient to prevent the system from accessing other isomers. This manifestation of broken ergodicity induced by the use of a (modified) QTB should also be kept in mind when using the method in systems with complex vibrational spectra.

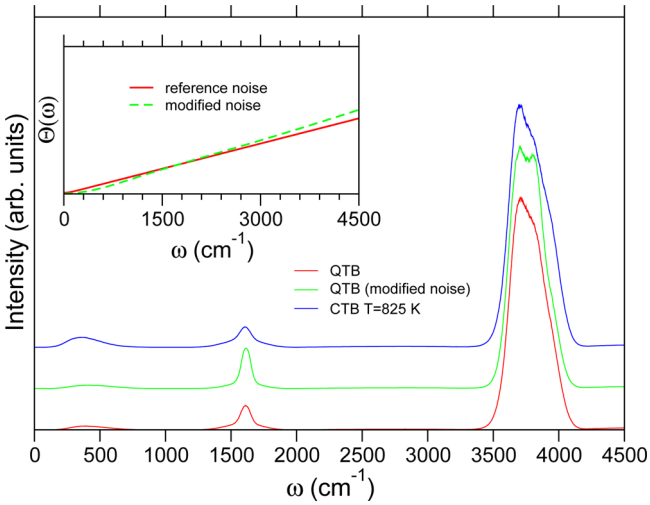

Figure 9. IR spectra obtained for the q-TIP4P/F water octamer at T = 50 K from classical molecular dynamics simulations with initial conditions drawn from CTB or QTB samplings. The inset shows an attempt of using an empirically altered noise power spectral distribution that maximizes the internal energy while minimizing δ.

The IR spectrum obtained by preparing the initial conditions with this modified noise function, shown in Figure 9, is barely distinguishable from the spectrum obtained with the original noise with PSD. This indicates that the spectral features and especially the excessive broadenings are not so much the consequence of the system visiting many multiple isomers, but

DOI: 10.1021/ct500678z
J. Chem. Theory Comput. XXXX, XXX, XXX−XXX

rather they reflect the intrinsically erroneous repartition of energy among modes. This result also shows that the simple procedure used here for modifying the noise based on global indicators is not sufficiently accurate for preventing leakage, and based on related work[32,40] we anticipate that more complex functions than those used above in (Section 3.3) would be required, if even successful for molecules.

Finally, further comments about the semiclassical treatment of nuclear motion in the QTB framework can be made by considering the equivalent classical thermodynamical state point. From the QTB trajectories the kinetic temperature of the particles is exceedingly high as it artificially compensates for the zero-point motion as a contribution stored in the classical momenta. This observation has lead previous authors to try to mimic nuclear quantum effects simply by injecting some kinetic energy in the system by the same amount as harmonic zero point energy, an approach known as quasiclassical molecular dynamics.[44] At the canonical temperature of 50 K, the equivalent classical temperature thus measured is close to 825 K. Performing the trajectories from classical initial conditions sampled at this temperature yields an IR spectrum also depicted in Figure 9, which again does not differ significantly from the two QTB spectra. This result confirms that the QTB method does not differ so much from the simple aforementioned semiclassical preparation scheme.

4. CONCLUDING REMARKS

Accounting for nuclear quantum effects in the simulation of many-body systems is generally desirable for weakly bound atoms or molecules or at low temperatures, as more than often vibrational delocalization affects thermodynamical but also transport or spectroscopic properties. QTBs relying on numerical solutions of the Langevin equation with correlated noise have recently emerged as one practical way of including those effects to a rather weak computational cost, making it comparable to standard classical simulations. They have been applied with some success to a variety of situations such as thermal conductivity[30−33] or spectroscopy[28,36] and even shock compression,[35] but they remain somewhat empirical with no strict guarantee of their validity even in low dimensionality.[42] Despite major computer advances, the method of QTBs remains appealing for its simplicity and generality. In the present article, we have challenged it over a set of systems exhibiting very different degrees of anharmonicities and delocalization, encompassing phase transitions and couplings between inter- and intramolecular modes.

In its portable version,[49] the QTB method is relatively free of empirical parameters and predicts energetics and zero-point shifts of rather good quality with respect to simple alternative estimates, especially at low temperature where usual PI methods become prohibitive. However, the method also appears to produce excessive spectral broadenings and, more importantly, can lead to wrong thermodynamical states as the result of major zero-point energy leakage issues. In particular, it works rather well for isolated molecules even in the context of spectroscopy or for weakly anharmonic solids but degrades as soon as the zero-point energy exceeds the lowest classical barriers, a situation likely occurring in molecular systems or atomic clusters. This contrasted performance originates from the intrinsic limitations of semiclassical preparation schemes that are best understood in the microcanonical ensemble, where the lack of quantum mechanical correlations between positions and momenta can artificially melt the system due to zero-point energy being converted into sufficient kinetic energy. Likewise it is not possible to use the QTB method to evaluate properties based on fluctuations such as the heat capacity, and one must then resort to applying the definition involving direct averages through noisy numerical derivatives. Our attempt to cure the leakage problem for the water octamer by modifying the generating noise through an empirical formula turned out to be inconclusive, despite keeping the system as rigid-like and preserving its internal energy within 15% of the targetted value, and it is likely that more refined dedicated strategies would be needed in general, with the additional drawback of likely being system (and temperature) dependent.

Based on the present results, and in the light of other recent investigations focusing on some of its fundamental properties,[38] we can conclude that the QTB method should be used as a semiclassical tool with its known limitations, thus with great caution especially for molecular systems where zero-point energy leakage issues are most stringent. The use of QTBs as an independent thermostatting procedure is therefore probably more recommendable for chemically homogeneous compounds[36] or as a way to assist PIMD simulations.[39]

■ ASSOCIATED CONTENT

Ⓢ Supporting Information

Comparison of internal energies obtained for the q-TIP4P/F water octamer using QTBs with different integrators, and influence of the damping constant and the Trotter discretization number on vibrational spectra. This material is available free of charge via the Internet at http://pubs.acs.org.

■ AUTHOR INFORMATION

Corresponding Author

*E-mail: jhrojas@ull.es.

Notes

The authors declare no competing financial interest.

■ ACKNOWLEDGMENTS

J. H.-R. acknowledges the financial support from Ministerio de Economía y Competitividad under grant no. FIS2013-41532-P and from Universidad de La Laguna. E.G.N. gratefully thanks the Dirección General de Investigación Científica y Técnica for financial support under grant nos. FIS2010-15502 and FIS2013-47350-C5-4-R. F.C. wishes to thank Prof. J.-L. Barrat and Dr. N. Bedoya-Martínez for useful discussions.

■ REFERENCES

(1) Gerber, R.; Ratner, M. *Adv. Chem. Phys.* **1988**, *70*, 97−132.
(2) Bowman, J.; Christoffel, K. M.; Tobin, F. *J. Phys. Chem.* **1979**, *83*, 905−912.
(3) Buch, V. *J. Chem. Phys.* **2002**, *117*, 4738−4750.
(4) Frantsuzov, P. A.; Mandelshtam, V. A. *J. Chem. Phys.* **2008**, *128*, 094304.
(5) Wang, H.; Sun, X.; Miller, W. H. *J. Chem. Phys.* **1998**, *108*, 9726−9736.
(6) Liu, J.; Miller, W. H. *J. Chem. Phys.* **2006**, *125*, 224104.
(7) Shao, J.; Makri, N. *J. Phys. Chem. A* **1999**, *103*, 7753−7756.
(8) Makri, N.; Nakayama, A.; Wright, N. *J. Theor. Comput. Chem.* **2004**, *3*, 391−417.
(9) Pollak, E.; Liao, J. L. *J. Chem. Phys.* **1998**, *108*, 2733−2743.
(10) Poulsen, J. A.; Nyman, G.; Rossky, P. J. *J. Chem. Phys.* **2003**, *119*, 12179−12193.
(11) Wang, C. Z.; Chan, C. T.; Ho, K. M. *Phys. Rev. B* **1990**, *42*, 11276−11283.

DOI: 10.1021/ct500678z
J. Chem. Theory Comput. XXXX, XXX, XXX−XXX

(12) Miller, W. H. *Proc. Natl. Acad. Sci. U.S.A.* **2005**, *102*, 6660−6664.
(13) Parrinello, M.; Rahman, A. *J. Chem. Phys.* **1984**, *80*, 860−867.
(14) Doll, J. D.; Coalson, R. D.; Freeman, D. L. *Phys. Rev. Lett.* **1985**, *55*, 1−4.
(15) Berne, B. J.; Thirumalai, D. *Annu. Rev. Phys. Chem.* **1986**, *37*, 401−424.
(16) Ceperley, D. M.; Mitas, L. *Adv. Chem. Phys.* **1996**, *93*, 1−38.
(17) Cao, J.; Voth, G. A. *J. Chem. Phys.* **1993**, *99*, 10070−10073.
(18) Hone, T. D.; Rossky, P. J.; Voth, G. A. *J. Chem. Phys.* **2006**, *124*, 154103.
(19) Craig, I. R.; Manolopoulos, D. E. *J. Chem. Phys.* **2004**, *121*, 3368−3373.
(20) Braams, B. J.; Manolopoulos, D. E. *J. Chem. Phys.* **2006**, *125*, 124105.
(21) Liu, J. *J. Chem. Phys.* **2014**, *140*, 224107.
(22) Wang, J.-S. *Phys. Rev. Lett.* **2007**, *99*, 160601.
(23) Heatwole, E. H.; Prezhdo, O. V. *J. Phys. Soc. Jpn.* **2008**, *77*, 044001.
(24) He, D.; Buyukdagli, S.; Hu, B. *Phys. Rev. E* **2008**, *78*, 061103.
(25) Buyukdagli, S.; Savin, A. V.; Hu, B. *Phys. Rev. E* **2008**, *78*, 066702.
(26) Bhattacharya, S.; Chaudhury, P.; Chattopadhyay, S.; Chaudhuri, J. R. *Phys. Rev. E* **2008**, *78*, 021123.
(27) Ceriotti, M.; Bussi, G.; Parrinello, M. *Phys. Rev. Lett.* **2009**, *103*, 030603.
(28) Dammak, H.; Chalopin, Y.; Laroche, M.; Hayoun, M.; Greffet, J.-J. *Phys. Rev. Lett.* **2009**, *103*, 190601.
(29) Ceriotti, M.; Bussi, G.; Parrinello, M. *J. Chem. Theory Comput.* **2010**, *6*, 1170−1180.
(30) Wang, J.-S.; Ni, X. X.; Jiang, J.-W. *Phys. Rev. B* **2009**, *80*, 224302.
(31) Savin, A. V.; Kosevich, Y. A.; Cantarero, A. *Phys. Rev. B* **2012**, *86*, 064305.
(32) Bedoya-Martínez, O.; Barrat, J.-L.; Rodney, D. *Phys. Rev. B* **2014**, *89*, 014303.
(33) Saaskilahti, K.; Oksanen, J.; Tulkki, J. *Phys. Rev. B* **2014**, *89*, 134301.
(34) Dammak, H.; Antoschenkova, E.; Hayoun, M.; Finocchi, F. *J. Phys.:Condens. Matter* **2012**, *24*, 435402.
(35) Qi, T.; Reed, E. J. *J. Phys. Chem. A* **2012**, *116*, 10451−10459.
(36) Calvo, F.; Nguyen-Thi, V.-O.; Parneix, P.; Falvo, C. *Phys. Chem. Chem. Phys.* **2012**, *14*, 10503−10506.
(37) Calvo, F.; Naumkin, F. Y.; Wales, D. J. *Chem. Phys. Lett.* **2012**, *551*, 38−41.
(38) Basire, M.; Borgis, D.; Vuilleumier, R. *Phys. Chem. Chem. Phys.* **2013**, *15*, 12591−12601.
(39) Ceriotti, M.; Manolopoulos, D. E.; Parrinello, M. *J. Chem. Phys.* **2011**, *134*, 084104.
(40) Ganeshan, S.; Ramirez, R.; Fernandez-Serra, M. V. *Phys. Rev. B* **2013**, *87*, 134207.
(41) Nava, M.; Ceriotti, M.; Dryzun, C.; Parrinello, M. *Phys. Rev. E* **2014**, *89*, 023302.
(42) Barrozo, A. H.; de Koning, M. *Phys. Rev. Lett.* **2011**, *107*, 198901.
(43) Dammak, H.; Chalopin, Y.; Laroche, M.; Hayoun, M.; Greffet, J.-J. *Phys. Rev. Lett.* **2011**, *107*, 198902.
(44) Varandas, A. J. C. *Int. Rev. Phys. Chem.* **2000**, *19*, 199−245.
(45) Habershon, S.; Manolopoulos, D. E. *J. Chem. Phys.* **2009**, *131*, 244518.
(46) Feynman, R. P.; Hibbs, A. *Quantum Mechanics and Path Integrals*; McGraw-Hill: New York, 1965.
(47) Wigner, E. P. *Phys. Rev.* **1932**, *40*, 749−759.
(48) Kirkwood, J. G. *Phys. Rev.* **1933**, *44*, 314−318.
(49) Barrat, J.-L.; Rodney, D. *J. Stat. Phys.* **2011**, *144*, 679−699.
(50) Calvo, F.; Doye, J. P. K.; Wales, D. J. *J. Chem. Phys.* **2001**, *114*, 7312−7329.
(51) Wales, D. J. *Mol. Phys.* **1993**, *78*, 151−171.
(52) Brünger, A.; Brooks, C. B.; Karplus, M. *Chem. Phys. Lett.* **1984**, *105*, 495−500.
(53) Mannella, R. *Phys. Rev. E* **2004**, *69*, 041107.
(54) Barker, J. A. *J. Chem. Phys.* **1979**, *70*, 2914−2918.
(55) Chandler, D.; Wolynes, P. G. *J. Chem. Phys.* **1981**, *74*, 4078−4095.
(56) Thirumalai, D.; Hall, R. W.; Berne, B. J. *J. Chem. Phys.* **1984**, *81*, 2523−2527.
(57) González, B. S.; Noya, E. G.; Vega, C. *J. Phys. Chem. B* **2010**, *114*, 2484−2492.
(58) Berry, R. S.; Beck, T. L.; David, H. L.; Jellinek, J. *Adv. Chem. Phys.* **1988**, *70*, 75−138.
(59) Pérez, A.; Tuckerman, M. E.; Müser, M. H. *J. Chem. Phys.* **2009**, *130*, 184105.
(60) Videla, P. E.; Rossky, P. J.; Laria, D. *J. Chem. Phys.* **2013**, *139*, 174315.
(61) Tuckerman, M. E.; Berne, B. J.; Martyna, G. J. *J. Chem. Phys.* **1992**, *97*, 1990−2001.
(62) Doye, J. P. K.; Wales, D. J. *J. Chem. Phys.* **1995**, *102*, 9659−9672.
(63) Calvo, F.; Doye, J. P. K.; Wales, D. J. *J. Chem. Phys.* **2001**, *115*, 9627−9636.
(64) Calvo, F.; Parneix, P.; Basire, M. *J. Chem. Phys.* **2009**, *130*, 154101.
(65) Presescu, C.; Sabo, D.; Doll, J. D.; Freeman, D. L. *J. Chem. Phys.* **2003**, *119*, 12119−12128.
(66) Frantsuzov, P. A.; Mandelshtam, V. A. *J. Chem. Phys.* **2004**, *121*, 9247−9256.
(67) Buch, V. A. *J. Chem. Phys.* **2002**, *117*, 4738−4750.
(68) Dykstra, C. E.; Shuler, K.; Young, R. A.; Bačić, Z. *J. Mol. Struct. (THEOCHEM)* **2002**, *591*, 11−18.
(69) Doye, J. P. K.; Miller, M. A.; Wales, D. J. *J. Chem. Phys.* **1999**, *111*, 8417−8482.
(70) Witt, A.; Ivanov, S. D.; Shiga, M.; Forbert, H.; Marx, D. *J. Chem. Phys.* **2009**, *130*, 194510.

DOI: 10.1021/ct500678z
J. Chem. Theory Comput. XXXX, XXX, XXX−XXX